THE ASTROPHYSICAL JOURNAL, 452:L57–L60, 1995 October 10

THE *IUE* MEGA CAMPAIGN: WIND STRUCTURE AND VARIABILITY OF HD 50896 (WN5)

NICOLE ST-LOUIS,[1] M. J. DALTON,[2] S. V. MARCHENKO,[1] A. F. J. MOFFAT,[1] AND A. J. WILLIS[2]
Received 1995 June 6; accepted 1995 July 18

ABSTRACT

We present preliminary results from an extensive study of UV line and continuum variability in the WN5 star HD 50896 = EZ CMa, monitored over 16 consecutive days in 1995 January, as part of the *IUE* "MEGA" campaign. Although variations are seen in all the major emission lines, the clearest occur in the unsaturated, subordinate N IV λ1718 line, and in the large number of Fe V/VI lines in the 1260–1450 Å region. These and the continuum variations are clearly locked into the 3.766 day period, which has been known for this star since 1980.

The observed variations suggest a global wind structure pattern that remains quite stable in the frame of the star, over the duration of the observations. This pattern is marginally compatible with that expected for the ionization cavity around an accreting neutron star companion in a 3.766 day W-R + NS binary. However, it can best be explained by some kind of corotating interaction regions emanating from hot (magnetically?) active regions near the surface of the stellar core. Such a model, although somewhat ad hoc, better accounts for the strong epoch-dependent variations seen in EZ CMa, as well as the fine structures seen in the global pattern.

Subject headings: stars: activity — stars: early-type — stars: mass loss — ultraviolet: stars

1. INTRODUCTION

HD 50896 (= EZ CMa = WR 6) is the sixth brightest and one of the best studied Wolf-Rayet (W-R) stars in the Galaxy. At optical wavelengths a 3.766 day period has been well established in photometric, polarimetric, and spectroscopic variability (see Robert et al. 1992 for a summary of its optical variability reported prior to 1991). However, the explanation of this modulation has yet to be agreed upon. Gosset & Vreux (1987) proposed another period at 1.255 days, but this was later shown by Antokhin et al. (1994) to correspond to the third harmonic of the 3.766 day period, and therefore that periodicity remains unique. Although phase-dependent changes are systematically observed in optical light, polarization, and line profiles, substantial epoch-to-epoch changes are also seen, where the pattern of the variations and shape of the curves generally differ from one set of observations to another—a very puzzling circumstance. Although HD 50896 is clearly a peculiar object, it is still uncertain whether its unusual variability is "pathological" or a reflection of a more general characteristic of W-R stars which, for some reason, is more prominent in this star.

In the ultraviolet, prior to the *IUE* MEGA campaign, HD 50896 has been the subject of three time-series studies. Willis et al. (1989) presented results from a 7 day *IUE* study in 1983, coupled to archival observations secured at sparsely separated intervals during 1978–1980. These data highlighted gross epoch-related changes in the pattern of its UV P Cygni profile variations, with the 1983 data showing little variability, compared to the large-scale variations apparent in earlier spectra. An *IUE* time series obtained over 6 days in 1988 showed modest level P Cygni profile variability, intermediate in amplitude between the earlier extremes (St-Louis et al. 1993). These data showed clear evidence for an ~1 day period in the profile variability, interpreted as arising in mechanisms intrinsic to the WN5 wind, and possibly comparable to that occurring in OB stars. An extensive *IUE* time series obtained in 1992, covering 5 days, revealed large-scale profile variability, similar to that seen in many of the early archival spectra (St-Louis et al. 1995). In these data, and to a lesser extent in the 1988 spectra, the 3.766 day periodicity is very evident.

In an attempt to explain the optical and UV variations observed in HD 50896, several models have been put forward, based on either a binary or rotational modulation effect. Radial and nonradial pulsations are generally excluded owing to the much shorter cycles expected and the lack of multiple periodicities. Arguments in favor of the binary (viz., WN5 + collapsar) hypothesis (see Firmani et al. 1980; Lamontagne, Moffat, & Lamarre 1986) are centered around evidence for a past supernova explosion: first, its runaway nature—HD 50896 is found at a distance of $z = 315$ pc below the Galactic plane (based on the most recent distance estimate, $d = 1.8$ kpc; Howarth & Schmutz 1995), potentially caused by the recoil action from the past explosion of a more evolved star, leading to a possibly still bound compact companion. Second, a supernova remnant (SNR) has been identified by Nichols-Bohlin & Fesen (1986) to be nearly centered on the same line of sight as HD 50896. However, the agreement between the radial distances of the star and the SNR is still controversial (Howarth & Schmutz 1995). Strong arguments in favor of the rotation-modulation hypothesis (i.e., intrinsic WN5 wind variations) include the epoch-dependent nature of its observed variability and the lack of strong X-ray emission: *ROSAT* and *Einstein* X-ray observations show $L_x \sim 3 \times 10^{32}$ ergs s^{-1} (Willis et al. 1994). If the WN5 star has a neutron star companion, the *emergent* X-ray luminosity from the source is expected to be a factor of ≥100 greater than observed (Stevens & Willis 1988). A working model of rotation modulation via enhanced jets was made by Matthews et al. (1992b). An inhomogeneous flattened wind was considered on the basis of polarimetric observations by Schulte-Ladbeck et al. (1990).

Previous *IUE* time-series studies of HD 50896 have been restricted to relatively short (~5–7 day) timescales. To make progress in understanding the variability in this star clearly

[1] Département de Physique, Université de Montréal, C.P. 6128, Succ. Centre Ville, Montréal, Québec, H3C 3J7, Canada; and Observatoire du Mont Mégantic.
[2] Department of Physics and Astronomy, University College London, Gower Street, London, England WC1E 6BT, UK.

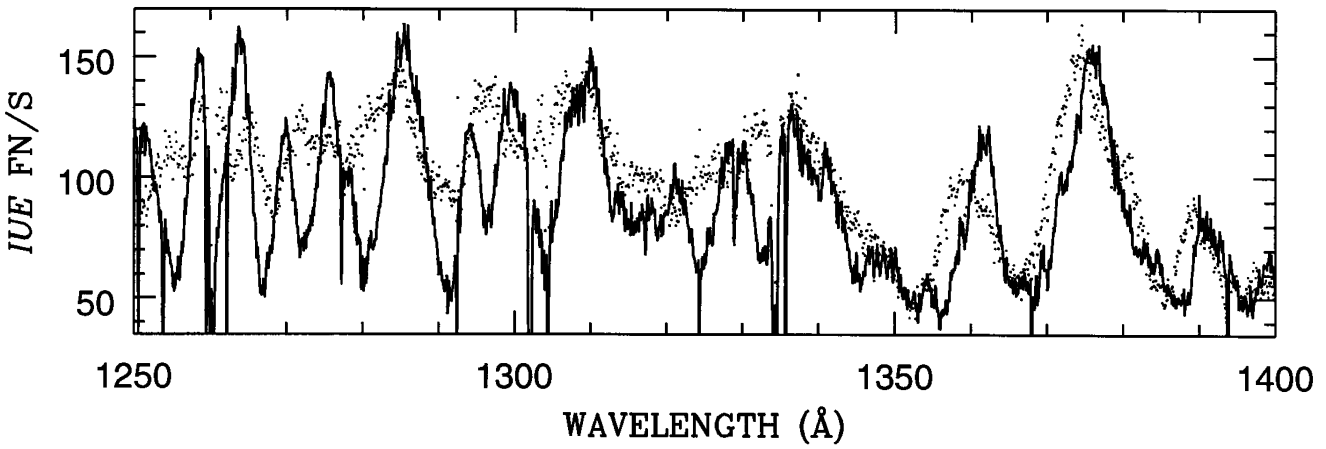

FIG. 2.—Plots of two extreme states of the wind for the region of concentration of Fe V/VI lines. Solid line refers to phase 0.70; dots refer to phase 0.20.

requires a longer monitoring time frame. With the *IUE* MEGA campaign, we have for the first time been able to investigate the variability of the source over several consecutive cycles in its 3.766 day period. The purpose of this Letter is to present preliminary results from these new data.

2. RESULTS

A gray-scale image representation of the *phase-dependent* variability observed in the N IV λ1718 P Cygni profile is shown in Figure 1 (Plate L14). A similar plot as a function of *time* is shown in Figure 1 in Paper I of this series (Massa et al. 1995). We make use of the N IV λ1718 line to illustrate the P Cygni profile variability in HD 50896, since this transition shows an unsaturated absorption component (unlike the C IV and N V resonance lines, which also have additional confusion effects as a result of their doublet nature) and is not overexposed in the emission peak (unlike He II λ1640). However, we emphasize that similar variability characteristics are also found in the P Cygni profiles of the C IV λ1550, N V λ1240, and Si IV λ1400 resonance lines, in the He II λ1640 transition, and in the large number of Fe V and Fe VI lines which occur in the λλ1260–1450 wavelength range (see Fig. 2).

From Figure 1 it is evident that two major types of P Cygni profiles are observed, embracing two main phase intervals in the 3.766 day period. The first, between approximately phases 0.50–0.85, shows a P Cygni absorption component with a violet edge extending to ~1900 km s^{-1}, a value which has been identified in the past with the terminal velocity v_∞ of the wind (St-Louis et al. 1993). We refer to this as the "quiet" state, since the profile and its variability characteristics are similar to those observed in our previous *IUE* studies, which showed relatively low-level changes. The second type of profile, which we term the "high-velocity" state, occurs essentially between phases 0.85–0.50 and shows enhanced absorption in the violet velocity range 1900–2900 km s^{-1} (i.e., higher than v_∞), accompanied by excess emission (or lack of absorption) at low negative velocities. This state shows more "structure" than the quiet state; two episodes can be identified (~0.95–0.05 and 0.2–0.3) in which the wind seems to move gradually back toward the quiet state and then go back suddenly to the high-velocity state.

Typical N IV λ1718 P Cygni profiles, reflecting these two distinct wind "states," are shown in the bottom panel of Figure 1. The peak of the emission also shows evidence for variability, albeit at a lower amplitude than in the absorption component. In general, at phases corresponding to the high-velocity state, the peak emission intensity is reduced. Compared to the blue side, only subtle changes (e.g., small excess at $\sim +v_\infty$ for phases $\phi \sim 0.15$–0.30) are seen in the red wing of the emission component.

In Figure 3 (Plate L15) we show a formal two-dimensional periodogram of the variations in the rectified N IV λ1718 P Cygni profiles. The 3.766 day period ($\nu = 0.266$) clearly dominates the periodogram, and we can also see the simple harmonics of this period at 2ν, 3ν, 4ν, 5ν, and 6ν, reflecting the fact that the variability does not follow a simple sinusoidal curve but has a more complex shape, in which power is leaked from the fundamental frequency into these higher harmonics. The intensity of the peak at $\nu = 1.059$ days^{-1} ($P = 0.944$ days) is at a level which is substantially higher than expected for a simple harmonic. Inspection of the overall time-series gray-scale data (Fig. 1) indicates that this is associated with the substructures seen at phases ~0.15, 0.35, 0.60–0.70, and 0.95.

The two lower panels to Figure 3 show the phase and amplitude of the sinusoid, for $\nu = 0.266$ days^{-1}, recovered from the "un-CLEANed" power spectrum. Note here the presence of prominent dips in Fourier power close to $v \sim -1700$ km s^{-1} and ~ -800 km s^{-1}, accompanied by a change of phase of about half a cycle between these two limits. These can be understood as pivot points between strong phase-dependent variations. A similar change in phase occurs on the red emission from $v \sim +1300$ km s^{-1} to $\sim +2200$ km s^{-1}, accompanied by much weaker pivots near each edge.

A comparison of the MEGA data for HD 50896 with our earlier *IUE* time series yields the following contrasts. The relatively nonvariable spectra obtained in 1983 look very similar to the present profiles in the quiet state. The 1988 data set showed modest changes with respect to the 1983 profiles (or the present quiet state) with the changes in the absorption component being confined to the -1900 to -3000 km s^{-1} velocity range. This is similar to what is observed here between the quiet and high-velocity states with two major differences. First, the level of variability was much smaller in 1988, and second, the high-velocity changes then were not accompanied by variations in the blue edge of the emission component, as is observed in the present data set. The variability observed in the 1992 data set over ~1 1/2 cycles is very similar, in amplitude and nature, to the present changes. Then, the two

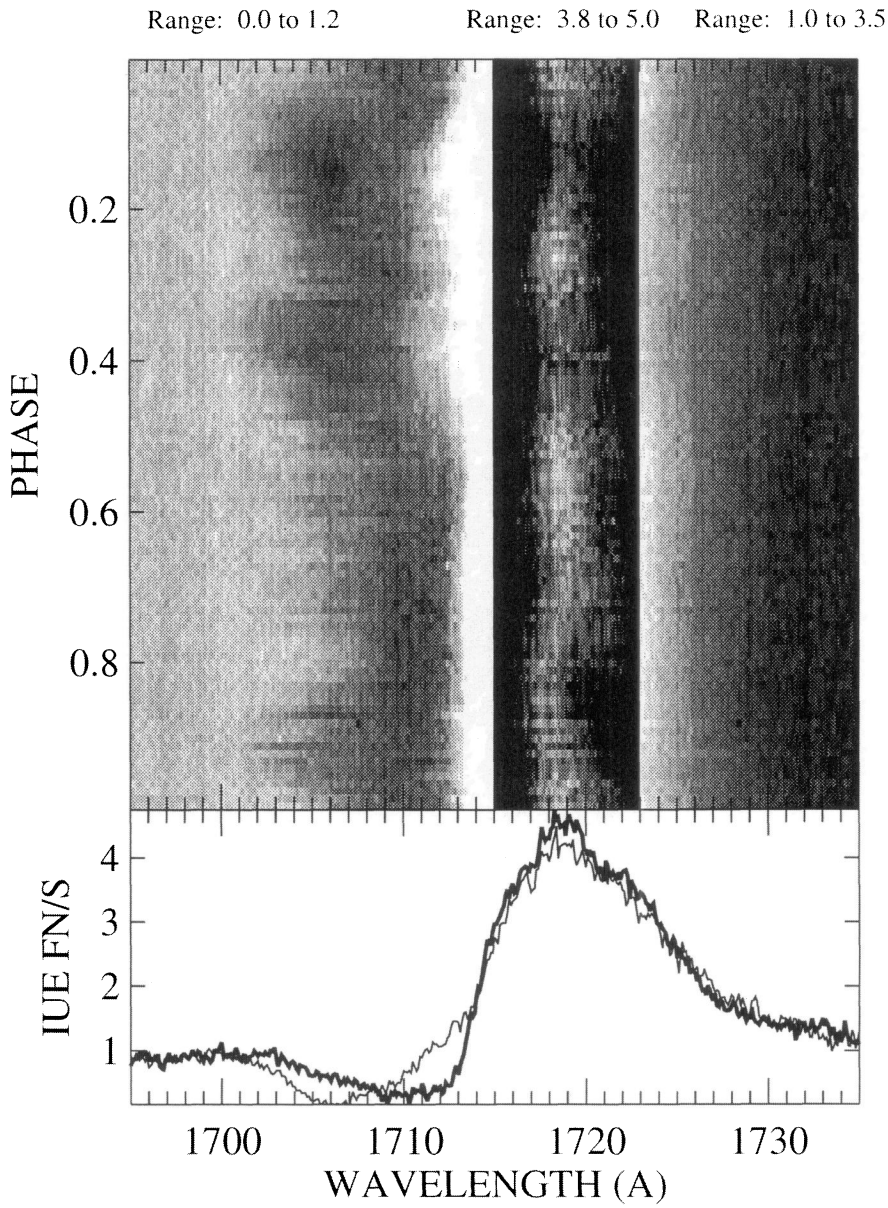

FIG. 1.—*Top*: Gray-scale plot of the N IV λ1718 line. Individual spectra were rectified in order to remove contributions from variability in the UV continuum. The data are displayed as a function of phase in the 3.766 day period, using the ephemeris given by Lamontagne et al. (1986), since we find that the major profile changes *are* locked into this period. The line profile has been divided into three wavelength sections, with different gray-scale level intervals displayed at the top, to bring out variability in different parts of the profile. *Bottom*: Two extreme states of the wind seen in the N IV λ1718 line.

ST. LOUIS et al. (see 452, L58)

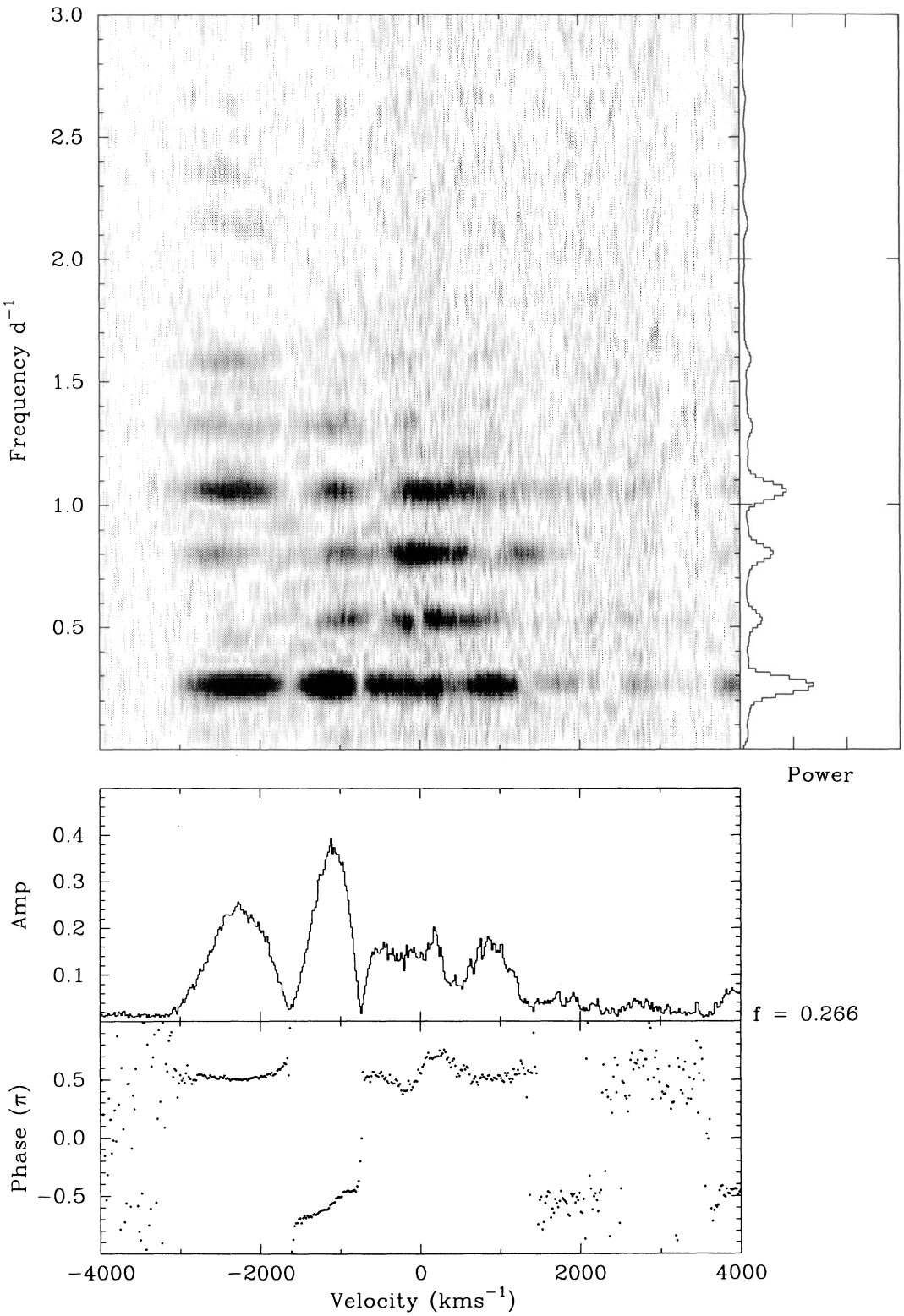

FIG. 3.—*Top*: Two-dimensional periodogram of the variations of the N IV λ1718 line. This has been formed by putting each spectrum into a three-dimensional data cube comprising wavelength (*X*-axis), time (*Y*-axis), and flux (*Z*-axis), with data from the cube, at each wavelength sample, then extracted into two-dimensional spectra in time and flux. Each of these spectra are then subjected to a Fourier CLEAN analysis (Roberts, Lehar, & Drehar 1987) to obtain a frequency vs. power spectrum at each wavelength. The "CLEANed" power spectra are then recombined into a single three-dimensional data cube as before, with the *Y*-axis now containing the frequency and the *Z*-axis containing the power. Darker regions show the frequencies at which significant power is found. *Bottom*: Phase and amplitude for the main period $P = 3.766$ days. The amplitude is merely a cut at $\nu = 0.266$ days^{-1} from the upper section.

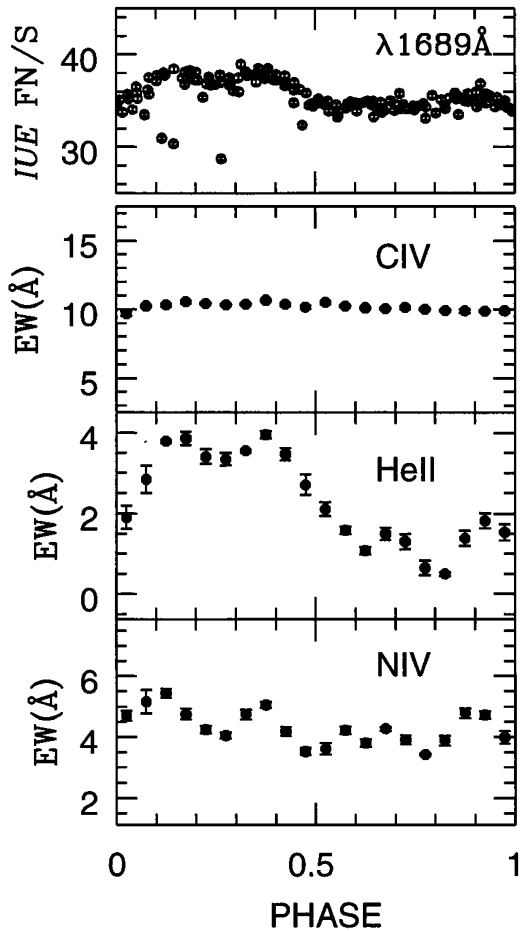

FIG. 4.—Phase plots of continuum flux and absorption component equivalent widths.

different wind states were observed but shifted in phase by ~0.2 compared to the present data set. For the two data sets to be consistent in phase requires an uncertainty in the Lamontagne et al. (1986) period of ~0.002–0.003 days, which is not excluded. Therefore, the nature and phasing of the changes could well be exactly the same in 1992 and 1995.

In Figure 4 we show the variability apparent in the MEGA data for the UV continuum in HD 50896 (*top panel*) measured as the mean intensity level in the λλ1680–1698 region, which is devoid of spectral features. Significant continuum variations (at the 5%–10% level) are apparent, which Fourier analysis show have the 3.766 day periodicity. We find that there is a striking correlation between the rectified line profile variations and the continuum variability, with the latter also showing the two distinct wind states. The UV continuum is higher when the high-velocity enhanced P Cygni absorption is apparent. The structure in the high-velocity state can also be identified in the UV continuum light curve and confirmed in a simultaneously obtained optical continuum light curve (Morel et al. 1995).

The lower three panels in Figure 4 show the P Cygni absorption equivalent widths for C IV, He II, and N IV, measured from -3000 km s^{-1} to the point where the absorption trough goes into emission. We have binned the data in intervals of 0.05 in phase for clarity. The ordinate scales were set to ±1.75 times the mean value of the equivalent width of each transition, to facilitate comparison. The 2 σ error bars (smaller than the size of the dots for C IV) indicate the internal error of the mean within one bin and therefore are probably conservative. The apparent constancy in the C IV measurements is somewhat misleading; the absorption trough is saturated over a wide velocity range, and the onset of high-velocity absorption enhancement is, roughly, balanced by a reduction in low-velocity absorption. In contrast, the He II and N IV absorption troughs are not black and are therefore amenable to more meaningful measurement. It is apparent that the relative amplitude of the He II variation is larger than in N IV, which may reflect the larger size of the He II line formation region in the WN5 wind. The He II and N IV data in Figure 4 show four clear peaks; this is a reflection of the fourth harmonic. Their position in phase is well correlated, but the width is slightly larger in He II, suggesting that the N IV line formation region has a shorter reaction time to any disturbance, which again may be a reflection of the different sizes of the line formation regions. As noted above, the overall pattern (two states) of line absorption variability seen in N IV, He II, and C IV is also apparent in the N V resonance doublet, and in the large number of Fe V/Fe VI lines present in the spectrum (Fig. 2). These species are expected to be formed over a large range of radii in the WN5 wind (Fe V and Fe VI especially close to the core), implying that the physical cause of the variability effects occupies a large fraction of the wind.

We have also measured the equivalent widths of the P Cygni emission components in C IV, He II, and N IV, from the crossover point in the absorption trough to $+3000$ km s^{-1} (avoiding the overexposed regions in He II λ1640). We find that the absorption and emission equivalent widths are anticorrelated in that, for all lines, a stronger absorption component is always accompanied by a reduced emission component. Note that the relative amplitude of emission variability is much less than absorption variability, e.g., for N IV EW(abs) = 4–6 Å, while EW(emis) = -32 to -36 Å. This coherency between the absorption and emission variability indicates that the linear scale of the material causing the variability is of the order of the size of the line formation regions. This is in contrast to our earlier conclusions based on the 1988 data (St-Louis et al. 1993), where no correlation was apparent between the emission and absorption equivalent width variations, and the physical linear scale was estimated to be of the order of the core radius of the star.

3. DISCUSSION

In Figure 5 we show a cartoon with a simple, schematic interpretation of the large-scale structure of the rotating wind of HD 50896 in 1995 January. The wind essentially divides up into two main sections: a fast wind (phases 0.05–0.50) and a slow wind (phases 0.50–1.05), with finer structure superposed. These structures rotate in a way that is strictly locked to the 3.766 day period during at least some four rotations. HD 50896 is either a binary or a single star with a globally structured wind, as we discuss briefly below.

3.1. *Binarity*

A complete lack of coherent phase-dependent sine-wave–like variations in radial velocity (RV) excludes the possibility that we are dealing with a high-mass companion (O or B star; massive stellar black hole). If it is a binary, it must have a low-mass, probably neutron star (NS) companion. In this case, any periodic RV variations of the W-R component are likely

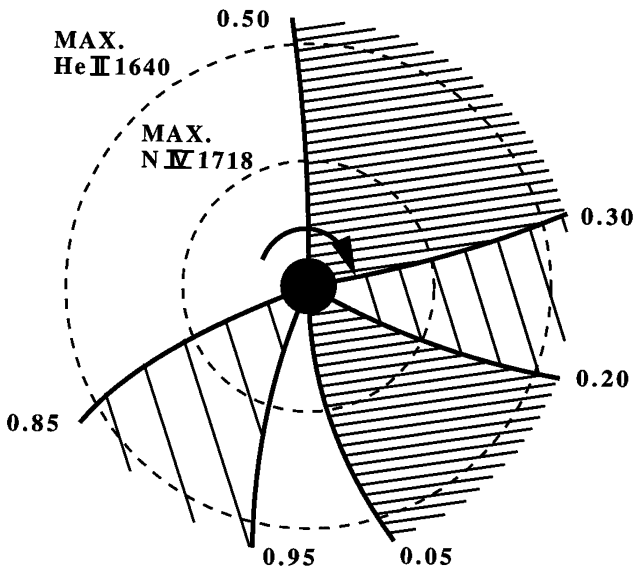

FIG. 5.—A cartoon showing our simple interpretation of the large-scale structure of the wind in EZ CMa based on the present UV observations. Heavy, light, or no shading refers, respectively, to the high-, intermediate-, or low-velocity wind. Phases are indicated along with the radii of maximum emission flux for two UV lines.

masked by line profile perturbations combined with low RV amplitude for a normal ~10–20 $M_\odot$ W-R star and a 1.4 $M_\odot$ NS. It is conceivable that accretion X-rays could be buried in the dense WR wind, although quantitative models *do* predict more copious X-ray emission than is observed (Stevens & Willis 1988).

The two observed main states of the W-R wind in the binary scenario must be caused by the ionizing effects of the NS companion. The NS must then be located on the side of the W-R star where the wind is in the "low" state; increased X-ray ionization there will lead to decreased wind acceleration (Blondin 1994). Also, on this heated side, electron scattering will be increased, leading to a minimum in the continuum light curve, as seen. On the opposite side, the wind is faster and we can look in deeper and thus to hotter layers; this would explain the color differences observed between the UV and optical light curves.

3.2. *Rotational Modulation*

The configuration in Figure 5 may be related to Mullan's (1984, 1986) picture of corotating interaction regions (CIRs) between fast- and slow-speed wind streams emanating from a single, rotating star. This model has been applied to O star winds more rigorously by Cranmer & Owocki (1995) in the context of accelerating dark absorption components (DACs) seen propagating outward in the P Cygni absorption edges.

In the case of HD 50896 and in the context of this model, we interpret the high-speed state as the perturbed state. In particular, there are four (two strong, two weak) regions from which a hotter wind emerges and produces a higher continuum flux level. This flux emerges mainly from near the visible base of the wind and is thus seen best when the region faces the observer (maximum light curve). In P Cygni lines, it is the absorption edges that show the largest amplitude variations, since such edges are formed by projection effect on the relatively small stellar core and the change between states occurs rapidly as the CIRs sweep by the line of sight to the core. The pure emission Fe V/VI lines must be formed in the inner wind region, so that they behave much like the continuum light curve. The delay in the change of state increases for lines of lower ionization level that are generally formed further out in the wind, as expected for CIRs that are dragged by momentum conservation as they propagate outward. If the creation of the active regions on the stellar surface is controlled by magnetic fields, it may be possible to observe such fields directly via Zeeman splitting, or indirectly via flare activity, as already claimed in the case of HD 50896 (Matthews, Moffat, & Marchenko 1992a). The lifetime of these active regions must be of the order of 5–10 rotations, before new ones appear and change the nature of the observed variability. However, in this context the similarity of the 1992 and 1995 patterns is curious.

The main advantage of the rotation modulation model over the binary model is that the epoch dependence of the variations becomes more plausible, and the fine structure of the perturbed wind finds a more natural, although somewhat ad hoc, explanation. As an extreme example, the near lack of UV variations in 1983 is difficult to explain by the W-R + NS binary model, in which there will always be some degree of ionization shadowing (Blondin 1994). Also, the binary model would have difficulty accounting for the systematic delay between lines of different ionization.

4. CONCLUSION

Although we cannot entirely exclude the possibility of a W-R + NS binary, the present UV observations combined with previous data favor a single-star model involving a rotation-modulated wind.

N. S. L., S. V. M., and A. F. J. M. are greatful to NSERC (Canada) and FCAR (Québec) for financial aid.

REFERENCES

Antokhin, I., Bertrand, J.-F., Lamontagne, R., & Moffat, A. F. J. 1994, AJ, 107, 2179
Blondin, J. M. 1994, ApJ, 435, 756
Cranmer, S. R., & Owocki, S. P. 1995, BAAS, 26, 1446
Firmani, C., Koenigsberger, G., Bisiacchi, G. F., Moffat, A. F. J., & Isserstedt, J. 1980, ApJ, 239, 607
Gosset, E., & Vreux, J.-M. 1987, A&A, 178, 153
Howarth, I. D., & Schmutz, W. 1995, A&A, 294, 529
Lamontagne, R., Moffat, A. F. J., & Lamarre, A. 1986, AJ, 91, 925
Massa, D., et al. 1995, ApJ, 452, L53 (Paper I in *IUE* MEGA series)
Matthews, J. M., Moffat, A. F. J., & Marchenko, S. V. 1992a, A&A, 266, 409
Matthews, J. M., St-Louis, N., Moffat, A. F. J., Drissen, L., Koenigsberger, G., Cardona, O., & Niemela, V. S. 1992b, in Nonisotropic and Variable Outflows from Stars, ed. L. Drissen, C. Leitherer, & A. Nota (San Francisco: ASP), 130
Morel, T., et al. 1995, in preparation
Mullan, D. J. 1984, ApJ, 283, 303
———. 1986, A&A, 165, 157
Nichols-Bohlin, J., & Fesen, R. A. 1986, AJ, 92, 642
Robert, C., et al. 1992, ApJ, 397, 277
Roberts, D. H., Lehar, J., & Drehar, J. W. 1987, AJ, 93, 968
Schulte-Ladbeck, R. E., Nordsieck, K. H., Nook, M. A., Magalhaes, A. M., Taylor, M., Bjorkman, K. S., & Anderson, C. M. 1990, ApJ, 365, L19
Stevens, I. R., & Willis, A. J. 1988, MNRAS, 234, 783
St-Louis, N., Howarth, I. D., Willis, A. J., Stickland, D. J., Smith, L. J., Conti, P. S., & Garmany, C. G. 1993, A&A, 267, 447
St-Louis, N., et al. 1995, in preparation
Willis, A. J., Howarth, I. D., Smith, L. J., Garmany, C. D., & Conti, P. S. 1989, A&A, 77, 269
Willis, A. J., Schild, H., Howarth, I. D., & Stevens, I. R. 1994, in Instability and Variability of Hot-Star Winds, ed. A.F.J. Moffat, S.P. Owocki, A.W. Fullerton, & N. St-Louis (Dordrecht: Kluwer), 321